

Original Paper

# PINK1/Parkin-Mediated Mitophagy Promotes Resistance to Sonodynamic Therapy

Lin Song Yongmin Huang Xuandi Hou Yaoheng Yang Shashwati Kala  
Zhihai Qiu Rui Zhang Lei Sun

Department of Biomedical Engineering, The Hong Kong Polytechnic University, Hong Kong SA, China

## Key Words

Sonodynamic therapy • Mitophagy • ROS • Mitochondrial dynamics • PINK1/Parkin signaling pathway

## Abstract

**Background/Aims:** Sonodynamic therapy (SDT), based on the synergistic effect of low-intensity ultrasound and sonosensitizer, is a potential approach for non-invasive treatment of cancers. In SDT, mitochondria played a crucial role in cell fate determination. However, mitochondrial activities and their response to SDT remain elusive. The purpose of this study was to examine the response of mitochondria to SDT in tumor cells. **Methods:** A human breast adenocarcinoma cell line - MCF-7 cells were subjected to 5-aminolevulinic acid (ALA)-SDT, with an average ultrasonic intensity of 0.25W/cm<sup>2</sup>. Mitochondrial dynamics and redox balance were examined by confocal immunofluorescence microscopy and western blot. The occurrence of mitophagy was determined by confocal immunofluorescence microscopy. **Results:** Our results showed that ALA-SDT could induce mitochondrial dysfunction through mitochondrial depolarization and fragmentation and lead to mitophagy. The Parkin-dependent signaling pathway was involved and promoted resistance to ALA-SDT induced cell death. Finally, excessive production of ROS was found to be necessary for the initiation of mitophagy. **Conclusion:** Taken together, we conclude that ROS produced by 5-ALA-SDT could initiate PINK1/Parkin-mediated mitophagy which may exert a protective effect against 5-ALA-SDT-induced cell death in MCF-7 cells.

© 2018 The Author(s)  
Published by S. Karger AG, Basel

## Introduction

The search for cancer treatment over the past 100 years has uncovered several major therapies such as surgery, chemotherapy, and radiotherapy [1, 2]. Although each of these options has provided significant benefits to patients, their limitations, such as low therapeutic efficiency and severe side-effects, have driven the search for more effective therapies [1-

4]. Sonodynamic therapy (SDT) has emerged as a promising alternative modality for cancer treatment [5, 6]. Sonosensitizers used in sonodynamic therapy usually show good tumor selectivity and the property of preferential accumulation in tumors. Combined with sonosensitizers, low intensity ultrasound could lead to cytotoxicity in tumors while leaving normal tissue undamaged and intact [7-12]. Unlike photodynamic therapy (PDT), which combines light and photosensitizer to achieve cell death to superficial tumors due to the limited penetration of laser light, ultrasound can be focused into deep tissues in three dimensions [13-15]. Hence, SDT has the advantage of being able to treat deep-seated cancer and focus on a small region to activate sonosensitizers in a site-directed manner. Though the mechanism of reactive oxygen species (ROS) generation during SDT treatment is not fully understood, still, it is commonly understood that ROS is responsible for cytotoxic effects of SDT. Several possible mechanisms such as acoustic cavitation, sonoluminescence have been proposed to explain the generation of ROS [11, 16, 17].

Although cancer cells obtain most of their energy through glycolysis, still, mitochondria serve as important signaling platforms in tumor progression [18, 19]. Mitochondria are dynamic organelles that continuously change their number and morphology through fission and fusion processes. Mitochondrial fusion and fission proteins are in charge of fusion-fission balance and the maintenance of mitochondrial morphology [20, 21]. This balance is known to be critical for overall cellular health. Mitochondria usually display a tubular or networked morphology under normal conditions. However, they undergo perinuclear clustering, preceded with mitochondrial fission and mitophagy when subjected to physiological stress. Fission events separate dysfunctional daughter mitochondria with low membrane potential, which are subsequently degraded by autophagosomes. Mitochondrial dysfunction is proposed to be responsible for the mitophagy [22-24]. However, the biological effects of SDT on mitochondria remains elusive.

Mitophagy is a regulated catabolic process whereby cells degrade their dysfunctional or damaged mitochondria to maintain a healthy mitochondrial population [25]. Mitophagy can thus alleviate cell injury and promote cellular homeostasis and survival. Mitophagy has been reported to be involved in tumor resistance to various cancer therapy by cleaning damaged mitochondria and maintaining healthy mitochondria [26, 27]. The PTEN-induced putative kinase 1 (PINK1) and Parkin signaling pathway are critically involved in mitophagy [28-30]. PINK1/Parkin pathway is in charge of priming damaged mitochondria for selective autophagic recognition. In healthy mitochondria, the level of PINK1 is low and it is constitutively imported to the inner mitochondrial membrane and degraded immediately. However, when mitochondrial membrane potential is dissipated, PINK1 stabilize on the outer membrane and forms a large complex on the outer membrane surface where it recruits Parkin to damaged mitochondria. In brief, mitochondrial depolarization results in high expression of PINK1 as well as subsequent recruitment of Parkin to the mitochondria. This unique regulation of PINK1 and Parkin allows the selective and efficient turnover of damaged mitochondria [28, 31, 32].

A large amount of evidence suggests that ROS contributes to mitochondrial dysfunction and cell apoptosis [33, 34]. ROS has been demonstrated to contribute to apoptosis and cell death in SDT [35-37]. Mitochondria are particularly vulnerable to damage as they are the main source and the targets of intracellular oxidative stress. In general, redox homeostasis ensures that cells respond properly under stress. Cells are equipped with antioxidant systems both in cytoplasm and mitochondria including free-radical scavengers Mn-superoxide dismutase (MnSOD) and Catalase to eliminate excessive ROS and maintain redox homeostasis [38, 39]. Excessive production of ROS could lead to organelle dysfunction, disturbed redox homeostasis and then induce apoptosis through a ROS-related mitochondrial pathway [40]. Specifically, selective mitochondrial autophagy, termed "mitophagy", may play a critical role in the process of cell death [41, 42]. However, mitochondrial dynamics and the mechanisms of mitophagy during SDT are not fully understood.

Given the important role of mitophagy in mitochondrial quality control and cell homeostasis, we hypothesize that mitochondrial dysfunction occurs and mitophagy is involved in 5-ALA-SDT treated MCF-7 cells. We investigated the roles and the molecular mechanisms of mitophagy during this process. We demonstrated that PINK1-Parkin mediated mitophagy plays a protective role in preventing apoptosis and cell death and the upstream role of ROS accumulation in this process.

## Materials and Methods

### *Reagents and antibodies*

Paraformaldehyde, bovine serum albumin (BSA), N-acetylcysteine (NAC), Diphenyleneiodonium chloride (DAPI) were purchased from Sigma-Aldrich. Goat anti-rabbit IgG-horseradish peroxidase (HRP), goat anti-mouse IgG-HRP were from Thermo Fisher Scientific (Carlsbad, CA, USA). Anti-GAPDH, and anti-LC3 polyclonal antibody were obtained from Sigma-Aldrich. Antibodies for anti-caspase-3, anti-caspase-9 were purchased from Cell Signaling Technology (Santa Cruz, CA, USA). Human Lamp-2 antibody was purchased from R&D (Minneapolis, MN, USA). PINK1 antibody was purchased from Novus Biologicals (Littleton, CO, USA). Anti-Parkin antibody was from Abcam (Cambridge, UK), LC3B polyclonal antibody, MFN1 polyclonal antibody, Catalase polyclonal antibody, SOD2 polyclonal antibody, and FIS1 polyclonal antibody were purchased from Thermo Fisher Scientific. Immunofluorescent secondary anti-rabbit/mouse IgG was from Jackson Immuno Research (West Grove, PA, USA).

### *Cell culture and Sonodynamic therapy*

The human breast adenocarcinoma cell line, MCF-7 cell line was purchased from Cell Bank of Type Culture Collection of Chinese Academy of Sciences (Shanghai, China). MCF-7 cells were maintained in Dulbecco's modified Eagle's medium (DMEM, Life Technologies, Carlsbad, CA, USA) supplemented with 10% fetal bovine serum (FBS, Life Technologies), 100 units/mL penicillin, and 100 µg/mL streptomycin. Cells were maintained at 37°C in a humidified chamber containing 95% air and 5% CO<sub>2</sub>. MCF-7 Cells at a confluence of 80% were digested with 0.25% trypsin for subculture. MCF-7 cells were divided randomly into four groups: (1) control, (2) ultrasound alone (ultrasound), (3) ALA alone, and (4) ALA plus ultrasound (SDT). 5-aminolevulinic acid (ALA) was obtained from Sigma (St Louis, MO, USA). It was dissolved in a PBS to a stock concentration of 1M and was stored in the dark at -20°C. ALA is a kind of classic agent belong to both sonosensitizers and photosensitizers. ALA can be converted to protoporphyrin IX (PpIX) within cells. ALA shows good tumor selectivity and could be used for tumor detection. For ALA-SDT treatment, ultrasound is needed to enhance the cytotoxic activities of ALA. For the ALA and ALA-SDT groups, the cells were incubated with 1mM ALA for a 4 h drug-loading time in DMEM medium supplemented with 10% FBS. After the treatment, the cells were cultured in fresh medium for further different hours (2h, 4h, 12h) and then prepared for different analyses.

### *Ultrasound System for SDT*

The cells in the SDT groups were exposed to a 1.0 MHz flat ultrasound transducer with a diameter of 35mm at an average intensity of 0.25W/cm<sup>2</sup>, burst mode with a pulse repetition frequency of 100Hz and duty cycle of 10% was applied for 10 min. The transducer was driven by a function generator (AFG 3251, Tektronix Company, Oregon, USA) connected to a power amplifier (Model 500A250C, RF Microwave Instrumentation, Souderton, PA, USA). The culture dish with cells was put on the top of a wave guide, 6cm away from the transducer, filled with water to facilitate transmission of ultrasound. The schematic diagram of the experimental setup was shown in Fig. 1A. We monitored the temperature change of water during the experiment and the data was shown in Fig. 1B. The temperature changed little during the experiment. The ultrasonic spatial peak temporal average intensity and 3-D distribution were measured by hydrophone (Onda Corporation, Sunnyvale, CA, USA) as shown in Fig. 1C, 1D.

#### Cell viability assay

Cell viability at different time points following ALA-SDT was determined using a Cell Counting Kit-8 (Sigma-Aldrich) according to the manufacturer's instructions. Briefly, Cells were plated at a density of 5000 cells per well in a 96-well plate and incubated in 100- $\mu$ L culture medium for 24h. Cytotoxicity was determined by adding 10  $\mu$ L CCK-8 reagent per well for 1 h at 37°C in 5% CO<sub>2</sub>. The absorbance of the treated samples against a blank control was measured at 450 nm as the detection wavelength. The viability of treated cells was determined by comparing to the untreated ones in the control group.

#### Apoptosis assay by flow cytometry

Cells were seeded at a density of  $5 \times 10^5$  cells in 6-cm dishes and incubated for 24h. Alexa Fluor 488 Annexin V/Dead Cell Apoptosis Kit (Thermo Fisher Scientific) was used to measure cell apoptosis at the different time point following ALA-SDT according to the manufacturer's instructions. Cells were collected and incubated with 5  $\mu$ L of the annexin V conjugate and 1  $\mu$ L of the PI working solution at room temperature for 15 minutes. The cells were analyzed by FACS Calibur flow cytometer and BD Accuri C6 Software (Becton-Dickinson, USA). The flow cytometry excitation wavelength is 488nm, the annexin V fluorescence is detected with a passband filter with a wavelength of 515nm, and a filter with a wavelength greater than 560nm is used to detect PI.

#### Detection of mitochondrial membrane potential

Mitochondrial membrane potential was measured using JC-1(Sigma- Aldrich). Briefly, cells were stained with 2.5 $\mu$ M JC-1 in the dark at 37°C for 30min and then washed with FACS buffer. The data was analyzed by FACS Calibur flow cytometer and BD Accuri C6 Software (Becton-Dickinson, USA). Excitation and emission settings were 488nm and 515-545nm (FL1 channel) for JC-1 monomers, 488nm and 564-606nm (FL2 channel) for JC-1 aggregates respectively.

#### ATP production assay

Cellular ATP production was measured by firefly luciferase-based ATP assay kit according to the manufacturer's instructions (Thermo Fisher Scientific). In brief, cells were lysed and centrifuged at 12000g for 5 min. 10 $\mu$ L of cell lysates were mixed with the 100 $\mu$ L ATP detection working solution in a 96-well white plate. The data was collected using BioTek Synergy Microplate Reader (BioTek Instruments Inc., Winooski, VT, USA). The protein concentration of cell lysates was determined by BCA assay kit. The data was evaluated by the ratio of cellular ATP level to the protein concentration.

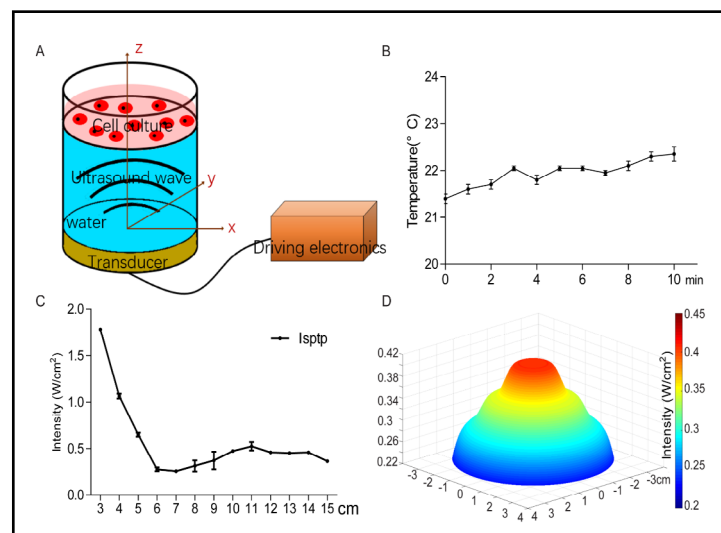


**Fig. 1.** Schematic diagram of SDT system. (A) The diameter of ultrasound transducer is 35mm. Water was filled between transducer and cell culture plate as ultrasound coupling. (B) The water temperature between transducer and cell culture plate were assessed with one minute interval for ten minutes during the sonodynamic therapy. Data represent the mean  $\pm$  SD based on 3 independent experiments. (C) Mean intensity of pulsed ultrasound was evaluated using ultrasonic hydrophone at different distances perpendicular to the transducer surface. Data represent the mean  $\pm$  SD based on 3 independent experiments. (D) Ultrasonic intensity distribution on vertical plane ( $Z=6$ cm). Data represent the mean  $\pm$  SD based on 3 independent experiments.

### *Determination of mitochondrial dynamics*

CellLight Mitochondria-GFP (Thermo Fisher) were used to track mitochondria according to the manufacturer's instructions. Briefly, Cells were incubated with the reagent overnight and mitochondria-GFP behavior can be observed in live cells. After treatment with ALA-SDT, cells were visualized under laser-scanning confocal microscopy with X63 objective (Nikon, Tokyo, Japan).

### *Immunofluorescence microscopy observation of mitophagy*

Mitophagy was determined by the co-localization of mitochondria with autophagosome and lysosomes following the standard guidelines [41].  $1 \times 10^5$  cells were seeded per 35mm confocal dishes (SPL Life Sciences, Korea) and incubated for 24h. After treatment, cells were stained with 100nM MitoTracker Deep Red (Thermo Fisher) at 37°C for 15 min. Cells were then washed with PBS and fixed with 4% PFA for 15min at room temperature. The fixed cells were further incubated overnight using antibodies against autophagosome marker LC3 or Lamp2 followed by Alexa Fluor 488- or 594-conjugated secondary antibody. The antibodies were diluted with 5% bovine serum albumin (Sigma). Nuclei were stained with DAPI for 10min at room temperature. Samples were observed by laser-scanning confocal microscopy with X63 objective (Nikon, Tokyo, Japan). 20-30 cells per condition were captured. The number of mitochondria co-localized with LC3 or Lamp2 was quantified.

### *Cell lysis and Western blot analysis*

To obtain cell lysates, the cells were washed with cold PBS and lysed for 10min on ice in a RIPA lysis buffer (50mM Tris-HCl, pH 7.4, 150mM NaCl, 1% NP-40, 0.5% sodium deoxycholate, 0.1% SDS) containing protease inhibitor mixture (Roche, Basel, Switzerland) and phosphatase inhibitor mixture (Roche) after treatment. After quantification and denaturation, the complexes were loaded in 10% polyacrylamide gels and transferred onto polyvinylidene difluoride (PVDF) membranes. Membranes were then blocked with 5% milk diluted in PBS containing 0.05% Tween 20 (PBST) for 1 h and then immunoblotted at 4°C overnight with the specified primary antibodies. After washing in PBST for three washes of 10min, membranes were incubated with relevant secondary anti-rabbit/mouse IgG at room temperature for 1 h. The membranes were treated with ECL reagents (Bio-rad, USA) before being visualized using a FluoChem E Imager (Protein-simple, USA). The density of protein band was quantified by Image J. GAPDH protein was used as an internal standard for SDI-quantification.

### *RNA interference*

Small interfering RNA (siRNA) duplexes were purchased from Thermo Fisher. The sequences of the Parkin oligonucleotides were: 5'-GAAUACAUCCCUACCUCAdTdT-3', 5'-GGCGCUAUUUGGCGCUUCAdTdT-3'. siRNA transfection was performed using Lipofectamine™ 2000 in accordance with the manufacturer's instructions. Briefly,  $1 \times 10^5$  cells were seeded per 35mm confocal dishes (SPL Life Sciences, Korea) and incubated for 24h. Cells were transfected with 20 μM synthesized siRNA targeting Parkin. The siRNA and Lipofectamine 2000 were separately diluted in serum-free DMEM and incubated for 5 min at room temperature. The two solutions were then gently mixed and incubated for 20 min, and then added to the cells. Inhibition of Parkin expression was observed 24h after transfection and the Parkin expression was analyzed by Western blot.

### *Determination of cellular and mitochondrial ROS production*

Intracellular ROS production was measured using DCFH-DA(Sigma-Aldrich). Briefly, 10 mM DCFH-DA diluted with DMEM were added to MCF-7 cells at 37°C for 20 min. Cells were then washed with PBS three times. Labeled cells were trypsinized and analyzed by flow cytometry. MitoSOX (Invitrogen, USA) was used to determine mitochondria-derived reactive oxygen species (mROS) production following the manufacturer's instructions. Cells were incubated with 10μM of mitoSOX at 37°C for 20 min. After washing with PBS three times, labeled cells were visualized by laser-scanning confocal microscopy with X63 objective (Nikon, Tokyo, Japan) and analyzed using Nikon NIS-Elements software.

*Statistical analysis*

Statistical analysis was performed with GraphPad Prism software. Image J, Photoshop CS, and Illustrator CS software were used for image processing following the general guidelines. All data, expressed as mean ± SD, were analyzed with a two-tailed student's *t*-test or by one-way ANOVA. *P*-values <0.05 were considered statistically significant.

**Results**

*ALA-SDT induced cytotoxicity and apoptosis*

To determine the cytotoxicity of ALA-SDT on MCF-7 cell lines, a CCK-8 assay was employed at different time points following SDT treatment. The results showed that either ALA alone or ultrasound alone groups could not induce obvious cytotoxicity, while ALA-SDT decreased cell viability of MCF-7 cells markedly by 25% and 32% at 4h and 12h following SDT, respectively (Fig. 2A, *p* < 0.05). We also investigated the effects of ALA-SDT on cell apoptosis. We found that ALA-SDT caused the apoptotic cell rate to increase to 10%,17% and 20% at 2h, 4h, and 12h following SDT respectively, compared to 3% in control group (Fig. 2B, *p* < 0.05). These data show that ALA-SDT inhibited cellular growth of MCF-7 cells in a time dependent manner. As a result, we selected 12h following ALA-SDT in the following experiments.

*ALA-SDT causes mitochondrial depolarization and fragmentation*

We then determined mitochondrial function, the main target of ALA-SDT treatment. As shown in Fig. 3A, ALA-SDT resulted in the aggregation of the JC-1 monomers from 17% of control cells to 59% in the SDT group indicating a significant decrease in mitochondrial membrane potential (*p* < 0.05). Meanwhile, ALA-SDT resulted in reduced production of ATP production from 11nmol/mg in control cells to 5.9nmol/mg in the SDT group (Fig. 3B, *p* < 0.05). To further study the effects of ALA-SDT on mitochondrial dynamics, images of mitochondrial morphology were taken and analyzed. Compared to control group, which contained long and tubular mitochondria, ALA-SDT group had increased punctate and short mitochondria and decreased tubular mitochondria (Fig. 3C and 3D). To determine the mechanisms by which ALA-SDT alters mitochondrial morphology in MCF-7 cells, we examined the expression of proteins that regulate mitochondrial fission and fusion. The results showed that ALA-SDT significantly decreased mitochondrial fusion protein (MFN1)

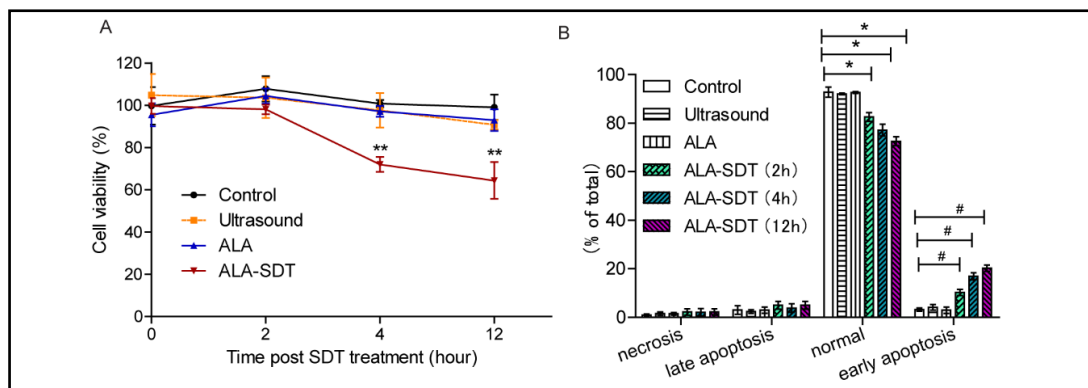


**Fig. 2.** Effects of ALA-SDT on cell viability and apoptosis. (A) In vitro cytotoxicity of ALA-SDT on MCF-7 cells was determined by CCK-8 assay. Data represent the mean ± SD based on 3 independent experiments. \*\**p*<0.01 vs. control. (B) Evaluation of cell apoptosis following ALA-SDT was done by flow cytometry through Annexin-V and propidium iodide (PI) double staining. The populations of early apoptotic cells (Annexin-V +/PI-) and late apoptotic cells (Annexin-V +/PI+) as a percent of total cells were evaluated. Data represent the mean ± SD based on 3 independent experiments. \**p*<0.05 vs. control.

**Fig. 3.** ALA-SDT induced mitochondrial dysfunction in MCF-7 cells. (A) Mitochondrial membrane potential was determined 2h post ALA-SDT treatment. Cells were stained with a JC-1 probe and the data were collected by flow cytometry. The percentage of JC-1 monomers were used to evaluate the mitochondrial potential. Data represent the mean  $\pm$  SD based on 3 independent experiments. \*\* $p < 0.01$  vs. control. (B) ATP production was measured 2h post ALA-SDT treatment by an ATP assay kit. Data represent the mean  $\pm$  SD based on 3 independent experiments. \*\* $p < 0.01$  vs. control. (C) Images of GFP-labeled mitochondria were captured upon exposure to ALA-SDT in MCF-7 cells. In the zoomed images, typical tubular mitochondria in control group and fragmented mitochondria in ALA-SDT group are shown. Representative images are shown in (C) with quantification data in (D). Data represent the mean  $\pm$  SD based on 3 independent experiments. \* $p < 0.05$  vs. control. Scale bar represents 10 $\mu$ m. (E, F) The protein expression level of mitochondrial fusion protein, MFN1, OPA1, and mitochondrial fission protein, FIS1 were determined by Western blot following ALA-SDT treatment. Representative images are shown in (E) with quantification data in (F). Data represent mean  $\pm$  SD of 3 independent experiments as determined by densitometry relative to GAPDH. \* $p < 0.05$  vs. control. ns, not significant.

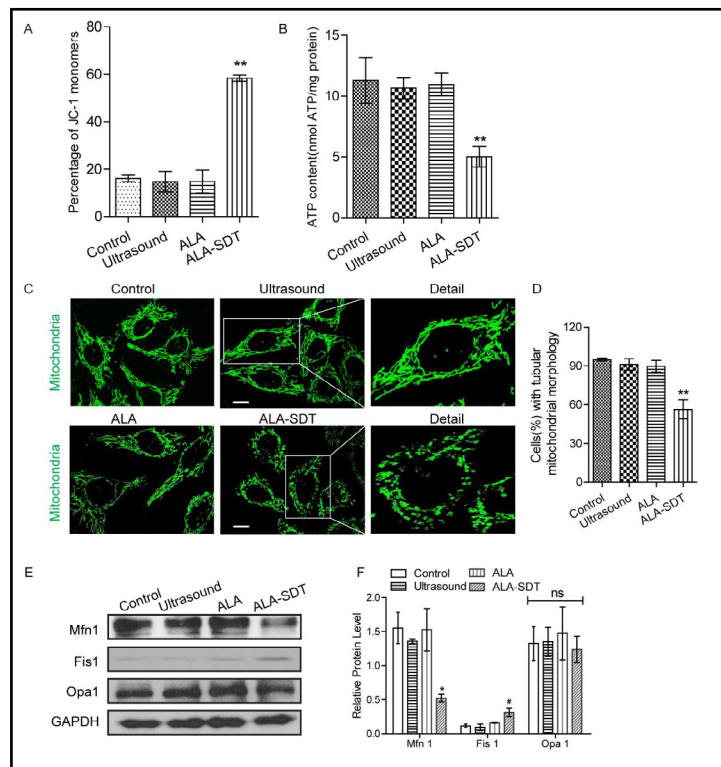


(Fig. 3E with quantification in Fig. 3F,  $p < 0.05$ ). Conversely, the expression of mitochondrial fission protein Fis1 increased dramatically following ALA-SDT treatment. The expression of Opa1 remained the same following ALA-SDT treatment. Together, these results suggest that ALA-SDT induced mitochondrial dysfunction and subsequent mitochondrial fission and fragmentation.

(Fig. 3E with quantification in Fig. 3F,  $p < 0.05$ ). Conversely, the expression of mitochondrial fission protein Fis1 increased dramatically following ALA-SDT treatment. The expression of Opa1 remained the same following ALA-SDT treatment. Together, these results suggest that ALA-SDT induced mitochondrial dysfunction and subsequent mitochondrial fission and fragmentation.

#### Mitophagy increases in ALA-SDT treatment

Increasing evidence suggests that mitophagy, a process of removal of damaged mitochondria through autophagy, is critical for maintaining proper cellular function. Since ALA-SDT resulted in mitochondrial dysfunction, we then explored whether mitophagy was induced during the process. We used universal markers LC3 and Lamp2 to stain autophagic vacuoles and lysosomes respectively and analyzed the co-localization of mitochondria and these acidic organelles (autophagosomes and lysosomes) as indicated by yellow fluorescence. As shown in Fig. 4A and 4B, ALA-SDT stimulated the co-localization of mitochondria with autophagosomes, with no co-localization in the control group. Similar results were obtained in Fig. 4C and 4D, where ALA-SDT resulted in the colocalization of mitochondria and lysosomes but not in the control group. Together, these results suggest the occurrence of mitophagy following ALA-SDT treatment.

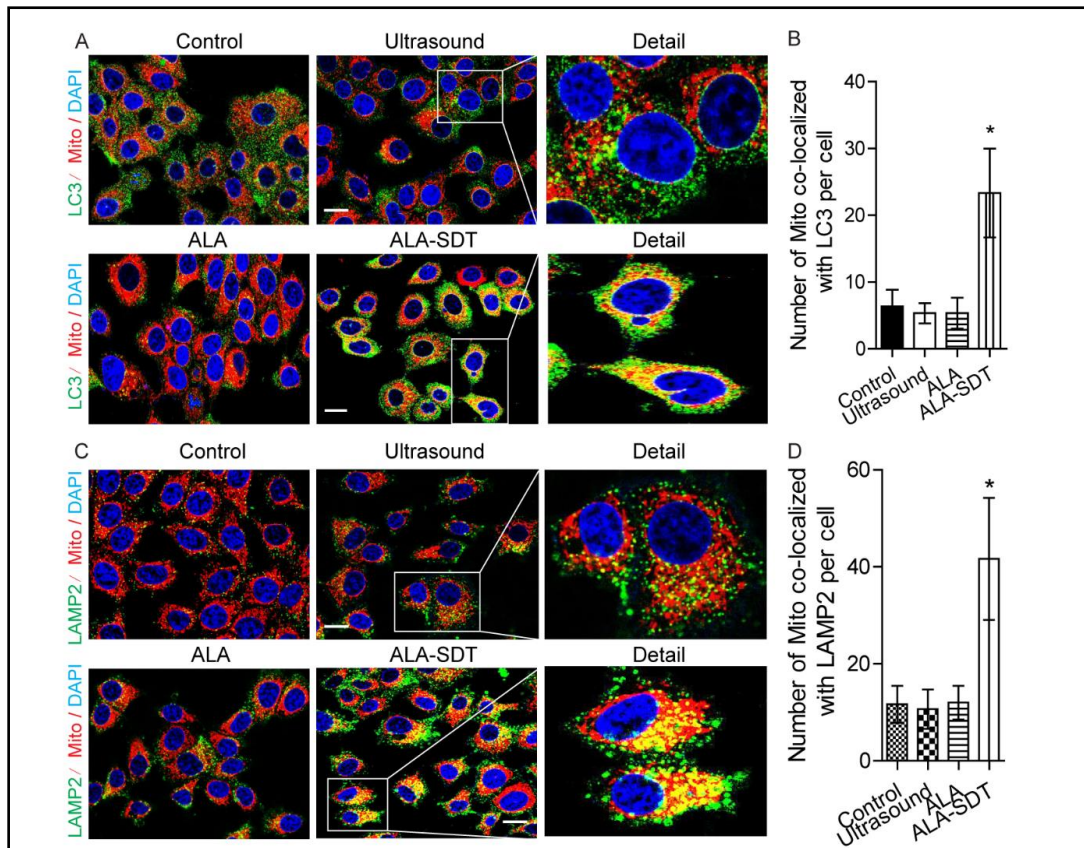


**Fig. 4.** ALA-SDT-induced mitophagy in MCF-7 cells. (A, B) MCF-7 cells were treated with ALA-SDT. Twelve hours later, treated cells were stained with mitochondrial marker Mitotracker and autophagy marker LC3. The number of mitochondria co-localized with LC3 per cell was quantified. At least 25 cells per experiment were analyzed. Representative images are shown in (A) with quantification data in (B). Data represent the mean  $\pm$  SD of three independent experiments. \* $p < 0.05$  in relation to control. (C, D) Twelve hours following ALA-SDT treatment, MCF-7 cells were stained with mitochondrial marker Mito and lysosome marker Lamp2. Representative images are shown in (C) with quantification data in (D). The number of co-localized lysosomes and mitochondria were measured from 25 cells in triplicate experiments. Data represent the mean  $\pm$  SD. \* $p < 0.05$  in relation to control. Scale bar represents 50  $\mu$ m.

#### *Parkin-dependent signaling pathway involved in ALA-SDT induced mitophagy*

Recent progress in mitophagy research has revealed that the PINK1-Parkin signaling is a key factor in mitophagy control. Hence, we then investigated whether the PINK1-Parkin signaling was involved in ALA-SDT-induced mitophagy. The results from the Western blot showed that ALA-SDT increased the expression level of PINK1, but not Parkin when compared to the control group (Fig. 5A with quantification in Fig. 5B,  $p < 0.05$ ). The localization of Parkin in MCF-7 cells was examined by immunofluorescent staining. We observed that in response to ALA-SDT, Parkin translocated significantly from cytoplasm to mitochondria in the peri-nuclear area when compared with the control (Fig. 5C with quantification in Fig. 5D). Taken together, these results indicated that PINK1-Parkin are involved in ALA-SDT induced mitophagy.

#### *Inhibition of mitophagy aggravated apoptosis and cell death induced by ALA-SDT*

To further determine the role of PINK1-Parkin mediated mitophagy on ALA-SDT-induced cell death, we used siRNA to knock down the Parkin in MCF-7 cells. Fig. 6A and 6B showed that silencing Parkin reduced by 25% of its normal level at 24h after transfection. Moreover, Parkin knockdown reduced ALA-SDT induced co-localization of mitochondria

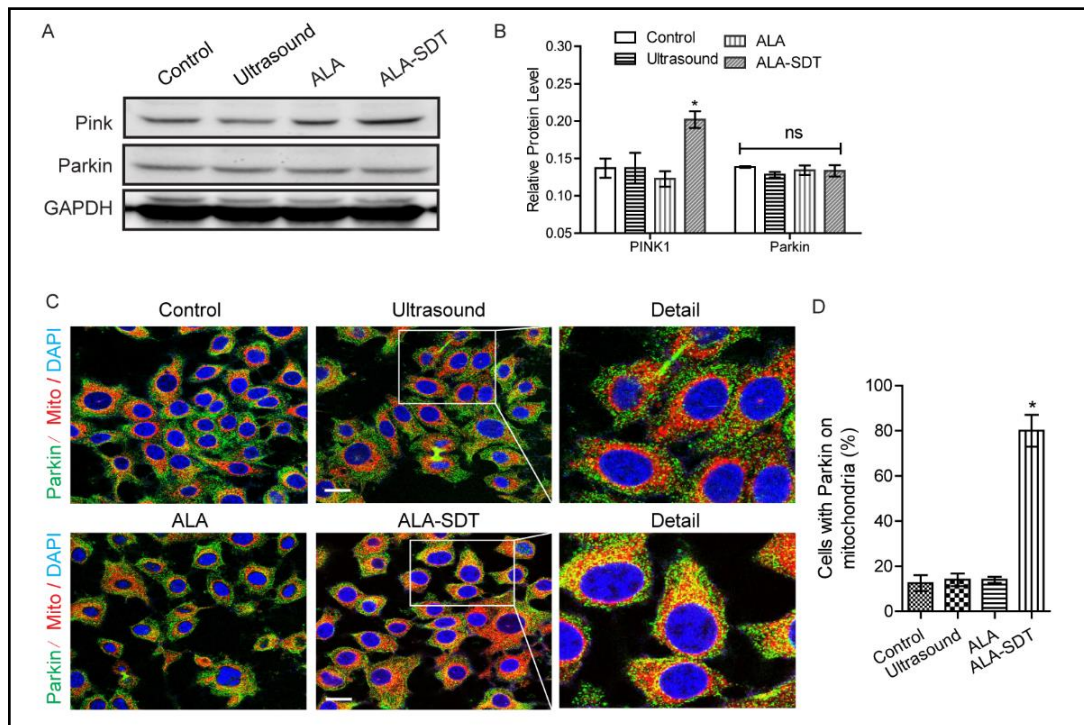


**Fig. 5.** PINK1/Parkin pathway is involved in ALA-SDT mediated mitophagy. (A, B) Twelve hours after ALA-SDT treatment, levels of PINK1 and Parkin were evaluated by Western blot. Representative images of blots and quantification from three independent experiments were shown in Fig. 4A, B. \* $p < 0.05$  vs. control. ns, not significant. (C, D) ALA-SDT-induced mitochondrial translocation of Parkin were determined by immunofluorescence. Cells were stained with Mitotracker (red) and anti-Parkin (green). Representative images are shown in (C) with quantification data in (D). At least 25 cells per experiment were analyzed. Quantification of fluorescence intensity of Parkin aggregates on the mitochondria were obtained from 3 independent experiments. \* $p < 0.05$  vs. control. Scale bar represents 50 $\mu$ m.

with lysosomes (Fig. 6C and 6D). These data indicate that Parkin knockdown inhibited the occurrence of mitophagy. We then examined the effects of PINK1-Parkin-mediated mitophagy on ALA-SDT induced cell death. As shown in Fig. 6E, compared to mock, Parkin knockdown induced a significant cell death response to ALA-SDT (20%,  $p < 0.05$ ,  $N = 5$ ). Consistent with cell viability, Parkin siRNA increased the apoptosis rate markedly by 10% compared with the mock group (Fig. 6F). These findings support a critical protective role of PINK1-Parkin-mediated mitophagy in preventing ALA-SDT-induced cell death.

#### *ROS contributed mitochondrial damage and subsequent mitophagy in ALA-SDT*

We further investigated the upstream regulatory mechanisms leading to mitochondrial dysfunction and subsequent mitophagy. There is increasing evidence that oxidative stress is responsible for mitophagy. Thus, we tested whether intracellular ROS and mitochondrial ROS increased following ALA-SDT treatment by flow cytometry. As shown in Fig. 7A and 7B, total intracellular ROS were significantly increased in MCF-7 cells 12h following ALA-SDT treatment compared with the control group. Similar trends were observed in mitoSOX-based detection of mitochondrial ROS (Fig. 7C and 7D,  $p < 0.05$ ,  $N = 3$ ). We also determined the expression of MnSOD and catalase by Western blot. Upon ALA-SDT treatment, the level of MnSOD was elevated, while little change of catalase was detected (Fig. 7E and 7F,  $p < 0.05$ ,  $N = 3$ ). To confirm the role of ROS in mitophagy in ALA-SDT, we treated MCF-7 cells with a ROS scavenger, N-acetyl-L-cysteine (NAC). Pretreatment with NAC showed a considerable blocking effect on the ALA-SDT-induced decrease of mitochondrial membrane potential (Fig. 7G,  $p < 0.05$ ,  $N = 3$ ). Consistent with this finding, NAC elevated ATP production of ALA-SDT

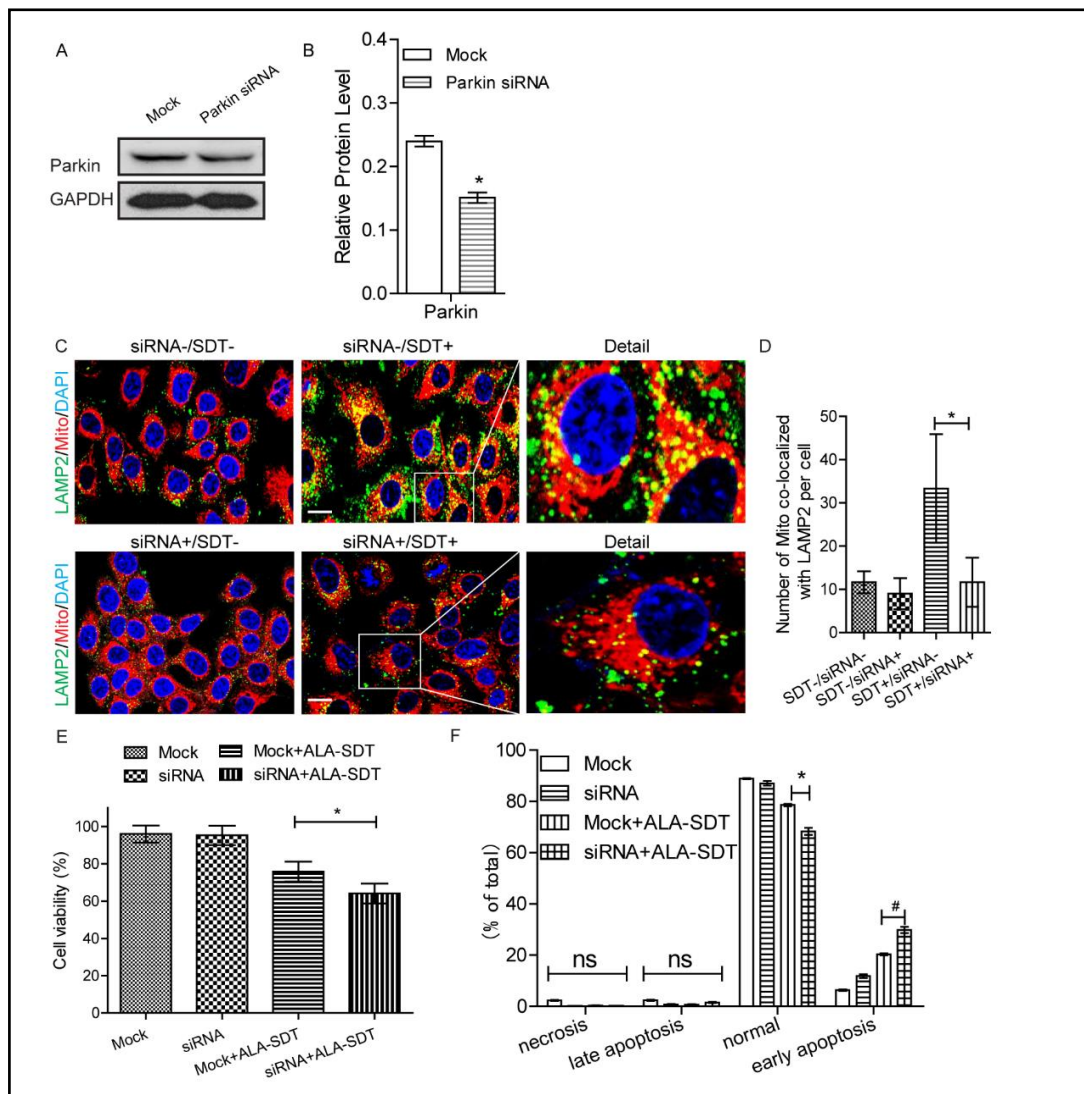
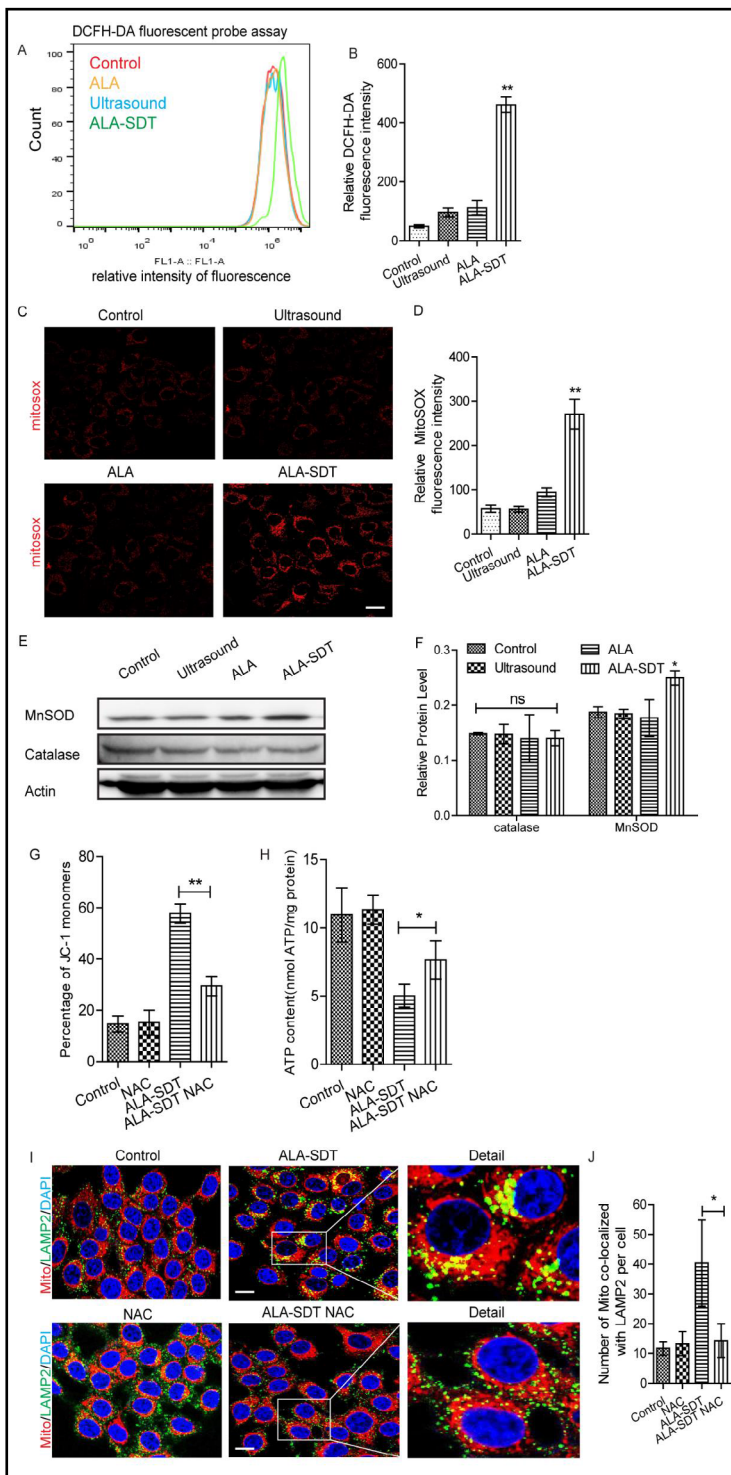


**Fig. 6.** The PINK1-Parkin pathway reduces ALA-SDT-induced cell death and apoptosis in MCF-7 cells. (A, B) MCF-7 cells were transfected with Parkin siRNA for 24h followed by ALA-SDT. Representative images showed the successful silencing of Parkin (A) with quantification data in (B). Quantitative analysis was from three independent experiments. \* $p < 0.05$  vs. control. (C-D) ALA-SDT-induced mitophagy in Parkin siRNA transfected MCF-7 cells was also determined using Lamp2 staining. Representative images are shown in (C) with quantification data in (D). At least 25 cells per experiment were analyzed. Quantitative analysis was from three independent experiments. \* $p < 0.05$  vs. control. Scale bar represents 50  $\mu$ m. (E, F) 12 hours after Parkin knockdown and ALA-SDT treatment, cell viability and cell apoptosis were measured. Data represent the mean  $\pm$  SD from three independent experiments. \* $p < 0.05$  vs. control.

group compared with control group (Fig. 7H,  $p < 0.05$ ,  $N = 3$ ). Moreover, the occurrence of mitophagy was almost completely inhibited by NAC. As shown in Fig. 7I and 7J, NAC pretreatment decreased the co-localization of mitochondria and lysosomes, which indicated a lower occurrence of mitophagy. These results demonstrated that the induction of ROS contributes to the initiation of mitophagy following ALA-SDT.

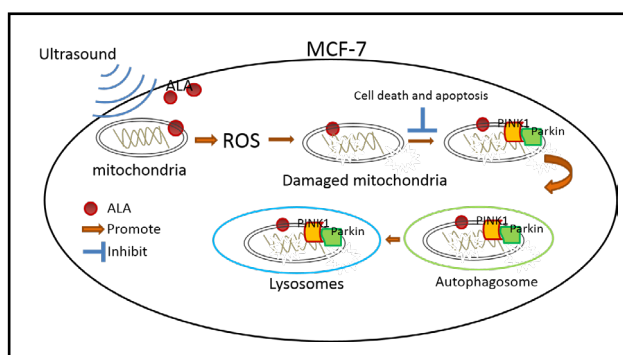
**Fig. 7.** Accumulation of ROS is critical for ALA-SDT-induced mitophagy. (A, B) Intracellular ROS were stained by DCFH-DA and analyzed by flow cytometry following by ALA-SDT. The values are the mean  $\pm$  SD of three independent experiments. **\*\*p**<0.01 vs. control. (C, D) Mitochondrial ROS were stained by mitoSOX and analyzed by flow cytometry following ALA-SDT. The values are the mean  $\pm$  SD of three independent experiments. **\*\*p**<0.01 vs. control. Scale bar represents 50 $\mu$ m. (E, F) MnSOD and catalase levels were evaluated by a Western blot. Representative images are shown in (E) with quantification data in (F). The values are the mean  $\pm$  SD of three independent experiments. **\*p**<0.05 vs. control. (G, H) Cells were pretreated with 1mM NAC overnight and then treated with ALA-SDT. Mitochondrial membrane potential and ATP production were determined respectively. The values are the mean  $\pm$  SD of three independent experiments. **\*p**<0.05 vs. control. **\*\*p**<0.01 vs. control. (I-J) The occurrence of mitophagy was determined using Lamp2 staining. Representative images are shown in (I) with quantification data in (J). The values are the mean  $\pm$  SD of three independent experiments. **\*p**<0.05 vs. control. Scale bar represents 50 $\mu$ m.



## Discussion

Mitochondria are fundamental regulators of cell function. Though cancer cells are relatively independent of mitochondrial oxidative pathways for ATP production, mitochondria still play a crucial role in regulating cellular homeostasis and cell death [43, 44]. Mitochondrial fission and fusion allow rapidly morphological changes in response to physiological and pathological conditions [45-47]. Dysfunction in mitochondrial dynamics is related to many

**Fig. 8.** A model for mitophagy activation by ALA-SDT. ROS generated by ultrasound activated ALA are the key factors for mitochondrial dysfunction, which triggers PINK1-Parkin mediated mitophagy activation. Moreover, increased apoptosis and decreased viability occurs when mitophagy is inhibited. Therefore, PINK1-Parkin mediated mitophagy plays a protective role in ALA-SDT-induced cell death.



neurodegenerative diseases, underpinning the role of fission and fusion in the maintenance of cellular homeostasis [46, 48, 49]. We observed that ALA-SDT could induce a decrease in mitochondrial membrane potential and ATP production, which means the initiation of mitochondrial dysfunction. ALA-SDT also triggers mitochondrial fragmentation mediated by mitochondrial fission. We observed the apparent morphology change of mitochondria from tubular mitochondrial network to punctate, fragmented mitochondria along with increased expression of mitochondrial fission protein FIS1, and decreased expression of mitochondrial fusion protein MFN1. Altogether, mitochondrial dysfunction was induced following ALA-SDT and lead to more fragmented mitochondria by fission.

It is well acknowledged that mitophagy is an important protective mechanism for selectively removing damaged mitochondria and preserving mitochondrial quality to meet metabolic demands [30, 42]. Dysfunctional mitochondria can trigger the occurrence of mitophagy. The PINK1-parkin pathway is the most well-documented signaling pathway in controlling mitophagy. Mutations in PINK1 or Parkin cause mitochondrial dysfunction and are directly related to Parkinson's diseases [50, 51]. In our study, a significant increase in colocalization of mitochondria and autophagosomes/lysosomes, increased expression of PINK1, as well as the translocation of Parkin from the cytoplasm to mitochondria showed that ALA-SDT induced significant mitophagy in cultured MCF-7 cells, which was involved in the activation of the PINK1-Parkin signaling pathway. Thus, PINK1-Parkin pathway, by promoting mitophagy, plays a crucial role in preserving healthy mitochondrial population.

An intricate crosstalk has been reported to exist between mitophagy, apoptosis and cell death [52, 53]. Usually, mitophagy is supposed to play a protective role in response to mitochondrial injury, removing damaged mitochondria. However, under certain circumstances, excessive mitophagy may induce over-degradation of mitochondria and subsequent irreversible cell death - autophagic cell death [54, 55]. In our study, Parkin knockdown decreased cell viability and increased the ratio of cell apoptosis, suggesting the protective role of mitophagy in protecting cells under ALA-SDT treatment. This implies the uncovered role of mitophagy in modulating the sensitivity of tumor cells to SDT and that drugs targeting mitophagy might improve the efficiency of ALA-SDT.

A number of studies have indicated the role of ROS in pathological conditions and its initiation of apoptosis [56, 57]. Mitochondria are the main target of ROS and are also considered to be the major source of ROS within the cell [58, 59]. We demonstrated that ALA-SDT induced the significant accumulation of both cellular and mitochondrial ROS, as well as the increased expression of cellular and mitochondrial anti-oxidative proteins. This indicated an oxidant-antioxidant imbalance occurs following ALA-SDT. ROS have been reported to cause mitochondrial dysfunction and activate multiple signaling pathways to induce mitophagy. In the present study, we used a ROS inhibitor, NAC, to decrease the level of intracellular and mitochondrial ROS and investigate their role in mitophagy in ALA-SDT. The NAC treatment significantly inhibited the decrease of the mitochondrial membrane potential and ATP production induced by ALA-SDT. Simultaneously, mitophagy induced by ALA-SDT

significantly decreased following the NAC treatment. These results suggest the accumulation of ROS induced by ALA-SDT is an important intracellular factor that contributes to triggering mitophagy.

In this study, we demonstrate that excessive intracellular ROS produced by ALA-SDT could induce mitochondrial dysfunction and lead to mitophagy. We also show that the PINK1-Parkin signaling pathway is involved in ALA-SDT-mediated mitophagy and plays a protective role in protecting mitochondrial functions and cell activities under oxidative stress (Fig. 8). To our knowledge, the present study is the first to systemically investigate the role of mitophagy in the process of ALA-SDT mediated cell death. These findings may apply to sonodynamic therapy mediated by other sonosensitizers and targeting mitophagy may improve the therapeutic efficiency of ALA-SDT as it is further examined and confirmed in clinical studies. As a relatively new modality for cancer treatment, more work still needed to be done before SDT is acceptable as a kind of major method for cancer treatment. Future studies are necessary to clarify the role of PINK-Parkin mediated mitophagy under different doses of SDT.

## Acknowledgements

The financial support from Research Grant Council through General Research Fund (project #15215615), and Natural Science Foundation of China through general program (project # 11674271) are greatly acknowledged.

## Disclosure Statement

The authors declare to have no competing interests.

## References

- 1 Baskar R, Lee KA, Yeo R, Yeoh KW: Cancer and radiation therapy: current advances and future directions. *Int J Med Sci* 2012;9:193-199.
- 2 Delaney G, Jacob S, Featherstone C, Barton M: The role of radiotherapy in cancer treatment: estimating optimal utilization from a review of evidence-based clinical guidelines. *Cancer* 2005;104:1129-1137.
- 3 DeVita VT, Jr, Chu E: A history of cancer chemotherapy. *Cancer Res* 2008;68:8643-8653.
- 4 Wyld L, Audisio RA, Poston GJ: The evolution of cancer surgery and future perspectives. *Nat Rev Clin Oncol* 2015;12:115-124.
- 5 Wan GY, Liu Y, Chen BW, Liu YY, Wang YS, Zhang N: Recent advances of sonodynamic therapy in cancer treatment. *Cancer Biol Med* 2016;13:325-338.
- 6 Wood AK, Sehgal CM: A review of low-intensity ultrasound for cancer therapy. *Ultrasound Med Biol* 2015;41:905-928.
- 7 Milowska K, Gabryelak T: Enhancement of ultrasonically induced cell damage by phthalocyanines *in vitro*. *Ultrasonics* 2008;48:724-730.
- 8 Cheng J, Sun X, Guo S, Cao W, Chen H, Jin Y, Li B, Li Q, Wang H, Wang Z, Zhou Q, Wang P, Zhang Z, Cao W, Tian Y: Effects of 5-aminolevulinic acid-mediated sonodynamic therapy on macrophages. *Int J Nanomedicine* 2013;8:669-676.
- 9 Dan J, Sun X, Li W, Zhang Y, Li X, Xu H, Li Z, Tian Z, Guo S, Yao J, Gao W, Tian Y: 5-Aminolevulinic Acid-Mediated Sonodynamic Therapy Promotes Phenotypic Switching from Dedifferentiated to Differentiated Phenotype via Reactive Oxygen Species and p38 Mitogen-Activated Protein Kinase in Vascular Smooth Muscle Cells. *Ultrasound Med Biol* 2015;41:1681-1689.
- 10 El-Sikhry HE, Miller GG, Madiyalakan MR, Seubert JM: Sonodynamic and photodynamic mechanisms of action of the novel hypocrellin sonosensitizer, SL017: mitochondrial cell death is attenuated by 11, 12-epoxyeicosatrienoic acid. *Invest New Drugs* 2011;29:1328-1336.

- 11 Hu Z, Fan H, Lv G, Zhou Q, Yang B, Zheng J, Cao W: 5-Aminolevulinic acid-mediated sonodynamic therapy induces anti-tumor effects in malignant melanoma via p53-miR-34a-Sirt1 axis. *J Dermatol Sci* 2015;79:155-162.
- 12 Li Y, Zhou Q, Deng Z, Pan M, Liu X, Wu J, Yan F, Zheng H: IR-780 Dye as a Sonosensitizer for Sonodynamic Therapy of Breast Tumor. *Sci Rep* 2016;6:25968.
- 13 Castano AP, Mroz P, Hamblin MR: Photodynamic therapy and anti-tumour immunity. *Nat Rev Cancer* 2006;6:535-545.
- 14 Mayor PC, Lele S: Photodynamic Therapy in Gynecologic Malignancies: A Review of the Roswell Park Cancer Institute Experience. *Cancers* 2016;8.
- 15 Zhang X, Liu T, Li Z, Zhang X: Progress of photodynamic therapy applications in the treatment of musculoskeletal sarcoma. *Oncol Lett* 2014;8:1403-1408.
- 16 Li Y, Zhou Q, Hu Z, Yang B, Li Q, Wang J, Zheng J, Cao W: 5-Aminolevulinic Acid-Based Sonodynamic Therapy Induces the Apoptosis of Osteosarcoma in Mice. *PLoS One* 2015;10:e0132074.
- 17 Tian F, Yao J, Yan M, Sun X, Wang W, Gao W, Tian Z, Guo S, Dong Z, Li B, Gao T, Shan P, Liu B, Wang H, Cheng J, Gao Q, Zhang Z, Cao W, Tian Y: 5-Aminolevulinic Acid-Mediated Sonodynamic Therapy Inhibits RIPK1/RIPK3-Dependent Necroptosis in THP-1-Derived Foam Cells. *Scientific Reports* 2016;6.
- 18 Zong WX, Rabinowitz JD, White E: Mitochondria and Cancer. *Mol Cell* 2016;61:667-676.
- 19 Bohovych I, Khalimonchuk O: Sending Out an SOS: Mitochondria as a Signaling Hub. *Front Cell Dev Biol* 2016;4:109.
- 20 Scatena R: Mitochondria and cancer: a growing role in apoptosis, cancer cell metabolism and dedifferentiation. *Adv Exp Med Biol* 2012;942:287-308.
- 21 Vasquez-Trincado C, Garcia-Carvajal I, Pennanen C, Parra V, Hill JA, Rothermel BA, Lavandro S: Mitochondrial dynamics, mitophagy and cardiovascular disease. *J Physiol* 2016;594:509-525.
- 22 van der Bliek AM, Shen Q, Kawajiri S: Mechanisms of mitochondrial fission and fusion. *Cold Spring Harb Perspect Biol* 2013;5. pii: a011072.
- 23 Scott I, Youle RJ: Mitochondrial fission and fusion. *Essays Biochem* 2010;47:85-98.
- 24 Youle RJ, van der Bliek AM: Mitochondrial fission, fusion, and stress. *Science* 2012;337:1062-1065.
- 25 Saito T, Sadoshima J: Molecular mechanisms of mitochondrial autophagy/mitophagy in the heart. *Circ Res* 2015;116:1477-1490.
- 26 Viale A, Pettazzoni P, Lyssiotis CA, Ying H, Sanchez N, Marchesini M, Carugo A, Green T, Seth S, Giuliani V, Kost-Alimova M, Muller F, Colla S, Nezi L, Genovese G, Deem AK, Kapoor A, Yao W, Brunetto E, Kang Y et al.: Oncogene ablation-resistant pancreatic cancer cells depend on mitochondrial function. *Nature* 2014;514:628-632.
- 27 Chourasia AH, Tracy K, Frankenberger C, Boland ML, Sharifi MN, Drake LE, Sachleben JR, Asara JM, Locasale JW, Karczmar GS, Macleod KF: Mitophagy defects arising from BNip3 loss promote mammary tumor progression to metastasis. *EMBO Rep* 2015;16:1145-1163.
- 28 Wu W, Xu H, Wang Z, Mao Y, Yuan L, Luo W, Cui Z, Cui T, Wang XL, Shen YH: PINK1-Parkin-Mediated Mitophagy Protects Mitochondrial Integrity and Prevents Metabolic Stress-Induced Endothelial Injury. *PLoS One* 2015;10:e0132499.
- 29 Zhang HT, Mi L, Wang T, Yuan L, Li XH, Dong LS, Zhao P, Fu JL, Yao BY, Zhou ZC: PINK1/Parkin-mediated mitophagy play a protective role in manganese induced apoptosis in SH-SY5Y cells. *Toxicol In vitro* 2016;34:212-219.
- 30 Kubli DA, Gustafsson AB: Mitochondria and mitophagy: the yin and yang of cell death control. *Circ Res* 2012;111:1208-1221.
- 31 Kawajiri S, Saiki S, Sato S, Sato F, Hatano T, Eguchi H, Hattori N: PINK1 is recruited to mitochondria with parkin and associates with LC3 in mitophagy. *FEBS Lett* 2010;584:1073-1079.
- 32 Geisler S, Holmstrom KM, Skujat D, Fiesel FC, Rothfuss OC, Kahle PJ, Springer W: PINK1/Parkin-mediated mitophagy is dependent on VDAC1 and p62/SQSTM1. *Nat Cell Biol* 2010;12:119-131.
- 33 Trachootham D, Lu W, Ogasawara MA, Nilsa RD, Huang P: Redox regulation of cell survival. *Antioxid Redox Signal* 2008;10:1343-1374.
- 34 Circu ML, Aw TY: Reactive oxygen species, cellular redox systems, and apoptosis. *Free Radic Biol Med* 2010;48:749-762.
- 35 Su X, Wang P, Yang S, Zhang K, Liu Q, Wang X: Sonodynamic therapy induces the interplay between apoptosis and autophagy in K562 cells through ROS. *Int J Biochem Cell Biol* 2015;60:82-92.

- 36 You DG, Deepagan VG, Um W, Jeon S, Son S, Chang H, Yoon HI, Cho YW, Swierczewska M, Lee S, Pomper MG, Kwon IC, Kim K, Park JH: ROS-generating TiO<sub>2</sub> nanoparticles for non-invasive sonodynamic therapy of cancer. *Sci Rep* 2016;6:23200.
- 37 Trendowski M: Using the Promise of Sonodynamic Therapy in the Clinical Setting against Disseminated Cancers. *Chemother Res Pract* 2015;2015:316015.
- 38 Candas D, Li JJ: MnSOD in oxidative stress response-potential regulation via mitochondrial protein influx. *Antioxid Redox Signal* 2014;20:1599-1617.
- 39 Gonzalez-Parraga P, Hernandez JA, Arguelles JC: Role of antioxidant enzymatic defences against oxidative stress H<sub>2</sub>O<sub>2</sub> and the acquisition of oxidative tolerance in *Candida albicans*. *Yeast* 2003;20:1161-1169.
- 40 Zheng X, Wu J, Shao Q, Li X, Kou J, Zhu X, Zhong Z, Jiang Y, Liu Z, Li H, Tian Y, Yang L: Apoptosis of THP-1 Macrophages Induced by Pseudohypericin-Mediated Sonodynamic Therapy Through the Mitochondria-Caspase Pathway. *Cell Physiol Biochem* 2016;38:545-557.
- 41 Ding WX, Yin XM: Mitophagy: mechanisms, pathophysiological roles, and analysis. *Biol Chem* 2012;393:547-564.
- 42 Kurihara Y, Kanki T, Aoki Y, Hirota Y, Saigusa T, Uchiumi T, Kang D: Mitophagy plays an essential role in reducing mitochondrial production of reactive oxygen species and mutation of mitochondrial DNA by maintaining mitochondrial quantity and quality in yeast. *J Biol Chem* 2012;287:3265-3272.
- 43 Vyas S, Zaganjor E, Haigis MC: Mitochondria and Cancer. *Cell* 2016;166:555-566.
- 44 Hsu CC, Tseng LM, Lee HC: Role of mitochondrial dysfunction in cancer progression. *Exp Biol Med* (Maywood) 2016;241:1281-1295.
- 45 Chen H, Chan DC: Emerging functions of mammalian mitochondrial fusion and fission. *Hum Mol Genet* 2005;14 Spec No. 2:R283-289.
- 46 Srinivasan S, Guha M, Kashina A, Avadhani NG: Mitochondrial dysfunction and mitochondrial dynamics-The cancer connection. *Biochim Biophys Acta* 2017;1858:602-614.
- 47 Ussakli CH, Ebaee A, Binkley J, Brentnall TA, Emond MJ, Rabinovitch PS, Risques RA: Mitochondria and tumor progression in ulcerative colitis. *J Natl Cancer Inst* 2013;105:1239-1248.
- 48 Iommarini L, Ghelli A, Gasparre G, Porcelli AM: Mitochondrial metabolism and energy sensing in tumor progression. *Biochim Biophys Acta* 2017;1858:582-590.
- 49 Caino MC, Altieri DC: Molecular Pathways: Mitochondrial Reprogramming in Tumor Progression and Therapy. *Clin Cancer Res* 2016;22:540-545.
- 50 Ryan BJ, Hoek S, Fon EA, Wade-Martins R: Mitochondrial dysfunction and mitophagy in Parkinson's: from familial to sporadic disease. *Trends Biochem Sci* 2015;40:200-210.
- 51 de Vries RL, Przedborski S: Mitophagy and Parkinson's disease: be eaten to stay healthy. *Mol Cell Neurosci* 2013;55:37-43.
- 52 Gump JM, Thorburn A: Autophagy and apoptosis: what is the connection? *Trends Cell Biol* 2011;21:387-392.
- 53 Zhang J: Autophagy and Mitophagy in Cellular Damage Control. *Redox Biol* 2013;1:19-23.
- 54 Kim I, Rodriguez-Enriquez S, Lemasters JJ: Selective degradation of mitochondria by mitophagy. *Arch Biochem Biophys* 2007;462:245-253.
- 55 Green DR, Levine B: To be or not to be? How selective autophagy and cell death govern cell fate. *Cell* 2014;157:65-75.
- 56 Di Meo S, Reed TT, Venditti P, Victor VM: Role of ROS and RNS Sources in Physiological and Pathological Conditions. *Oxid Med Cell Longev* 2016;2016:1245049.
- 57 Ling YH, Liebes L, Zou Y, Perez-Soler R: Reactive oxygen species generation and mitochondrial dysfunction in the apoptotic response to Bortezomib, a novel proteasome inhibitor, in human H460 non-small cell lung cancer cells. *J Biol Chem* 2003;278:33714-33723.
- 58 Schieber M, Chandel NS: ROS function in redox signaling and oxidative stress. *Curr Biol* 2014;24:R453-462.
- 59 Mao X, Yu CR, Li WH, Li WX: Induction of apoptosis by shikonin through a ROS/JNK-mediated process in Bcr/Abl-positive chronic myelogenous leukemia (CML) cells. *Cell Res* 2008;18:879-888.